Ausforming of Medium Carbon Steel

Seung-Woo Seo [a] Geun-Su Jung [a] Jae Seung Lee [b]
Chul Min Bae [b] H. K. D. H. Bhadeshia [a,c] Dong-Woo Suh [a]

[a] *Graduate Institute of Ferrous Technology, Pohang University of Science and Technology, Pohang 790-784, Republic of Korea*

[b] *Technical Research Laboratories, POSCO, Pohang 790-785, Republic of Korea*

[c] *Materials Science and Metallurgy, University of Cambridge, CB2 3QZ, U.K.*

Abstract

The prospect of enhancing the hardness of low-alloy steel for the manufacture of fasteners is examined using ausforming, in which the austenite is deformed rapidly at a low temperature to increase its dislocation density prior to quenching in order to obtain the harder martensite. Surprisingly small deformations accomplish large gains in hardness and the dislocation density of martensite, with diminishing returns at larger deformations. The main contribution to the hardness has been identified as the extra dislocations inherited by the martensite from the deformed austenite, rather than the refinement of microstructure by the ausforming process. Clear evidence is reported for the mechanical stabilisation of the austenite due to ausforming. Tempering heat-treatments tend to diminish the advantages of ausforming.

Key words: ausforming, steel for fasteners, martensite, mechanical stabilisation

1 Introduction

There are essentially two domains in a time-temperature-transformation diagram, identified by two C-curves, the top curve corresponding to reconstructive transformations and the lower one to displacive reactions. Between these two C-curves, there is a range of temperatures $\approx 550 - 600\,^{\circ}\mathrm{C}$, where the transformation of austenite takes a much longer time; as a consequence, this region of the TTT diagrams is often referred to as a 'bay'. Thus, the metastable austenite in the bay can be plastically deformed without inducing phase transformation, so that any martensite obtained on cooling to ambient temperature has a larger defect density, is finer in scale and may be reinforced with substitutionally-alloyed carbides. Such a process is known as ausforming [1–

4]. The deformation is conducted at relatively low temperatures where the recrystallisation of austenite does not occur and even recovery is minimal.

In the past, much of the work on ausforming has been conducted on richly-alloyed steels in order to obtain sufficient time within the bay to permit deformation. Work on low-alloy steels has involved austenite deformation at high temperatures in the non-recrystallisation region ($> 900\,°\mathrm{C}$) [5]. However, in certain applications, such as in the production of fasteners, it is possible to implement rapid deformation prior to quenching. In such cases it may be feasible to ausform low-alloy steels and gain hardness together with structural refinement by deformation in the bay of the TTT diagram. The advantage of the lower-temperature deformation would be to substantially enhance the hardness. The aim of the present work was, therefore, to investigate the ausforming of a low-alloy steel destined for the manufacture of fasteners.

2 Experimental Methods

The alloy studied is Fe-0.36C-0.74Mn-0.23Si-1.0Cr-0.21Mo wt%, a cold-heading quality steel used ultimately in the quenched and tempered martensitic condition. A 50 kg ingot was vacuum-melted and then hot-rolled into 30 mm plate with a finishing rolling temperature above $900\,°\mathrm{C}$. Cylindrical samples with 3 mm diameter and 10 mm length were machined for dilatometric experiments conducted on a Thermecmastor-Z machine made by Fuji Electronic Industrial Co. Ltd. The temperature that is reported from these experiments corresponds to measurements made at the central position along the compression axis, where metallographic observations and hardness measurements were also conducted. This mitigates the effects of any temperature variation along the length of the sample. Austenitisation was at $880\,°\mathrm{C}$ for 60 min. Fig. 1 compares the isothermal transformation behaviour against AISI 4140 steel which has similar composition [6]. There is a bay around $600\,°\mathrm{C}$ which should help with the ausforming process.

Ausforming was studied using 8 mm diameter and 12 mm length cylindrical samples compressed at 500 or $600\,°\mathrm{C}$ on a thermo-mechanical simulator, with nominal reduction ratios of 10, 30 and 50% at a strain rate of $10\,\mathrm{s}^{-1}$, followed by quenching to obtain martensite. The samples were further tempered at $550\,°\mathrm{C}$ for 90 min; the metallography of these samples was conducted on the longitudinal section. The strain analysis was conducted using the finite element method implemented on ABAQUS, with materials properties of SCM435 steel which has a similar composition to the investigated alloy [8]. The friction coefficient was taken to be 0.366, evaluated from the geometry of the deformed cylinders [9].
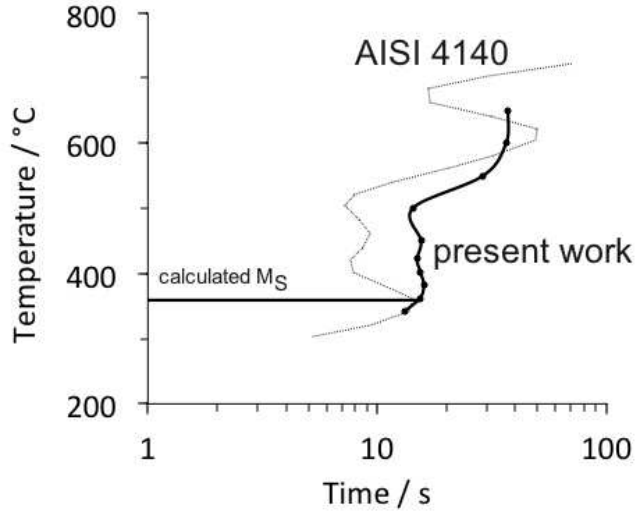
Fig. 1. Time-temperature-transformation diagram showing the onset of transformation. The austenitisation temperature was 880 °C for the alloy studied here and 860 °C for the AISI 4140 steel. The martensite-start temperature was calculated as in [7].

Vickers hardness was measured using a 1 kgf load; the quoted values represent averages of five measurements. Microstructures were observed using optical and scanning electron microscopy (SEM) with electron back-scatter diffraction (EBSD). Samples for optical microscopy were etched using 2% nital. EBSD measurements required final polishing with colloidal silica in order to reduce any effects of surface deformation during sample preparation. Precipitated carbides were examined by transmission electron microscopy with samples extracted using focused-ion beams. The dislocation density was measured using X-ray diffraction analysis of peak broadening [10, 11], using samples chemically polished in 4% HF in H_2O_2, which removed more than 100 µm of material from the surface. Monochromated $Cu\,K_\alpha$ radiation was used to capture the 110_α, 200_α, 211_α, 220_α, 310_α, and 222_α peaks. Scanning was over the range $2\theta = 40 - 145°$, with a step size of $0.01956°$ and with 2 s per step. After shape correction, the peaks were fitted into Psudo Voight function to extracting full-width, half-maximum (FWHM) and Fourier coefficients. The instrumental effect was eliminated by Stokes method [12], then the dislocation density was calculated by using the modified Williamson-Hall and Warren-Averbach methods, as described in [10].

3 Cooling curves and strain distribution

Cooling curves were recorded from samples that were made austenitic at 880 °C, cooled to 600 °C at an average rate of $\approx 45\,°C\,s^{-1}$ for ausforming and then cooled to ambient temperature. The curves exhibit deviations from from the general trend at temperatures below 300 °C, due to the latent heat of martensitic transformation, Fig. 2a. The martensite-start (M_S) temperature of the steel is 355 °C. It is evident that martensite forms at a lower temperature as the nominal reduction ratio is increased, a reflection of an effect known classically as mechanical stabilisation [13–21]. In this, the dislocation debris

3

in the deformed austenite interferes with the passage of the transformation interface, thus rendering it sessile. The phenomenon is associated uniquely with displacive transformations [22] because where the transformation interface must be glissile in order to propagate without the need for diffusion.

Fig. 2b shows the effective strain [1] distribution on the cylinder axis along the length of the compressed sample; it should be noted that all the metallographic observations were made at the mid-point of the axis. The strain is naturally concentrated in the middle of the sample, where all of the microstructural characterisations were performed. The maximum strain was 0.17, 0.7 and 1.7 corresponding to the nominal reduction ratios of 10%, 30% and 50%.

4   Microstructure and hardness

Metallographic studies have been carried out for all the samples, but the most significant micrographs are presented in Fig. 3. The optical and scanning electron micrographs for the sample deformed to a nominal strain of 50% at 500 °C has a significant amount of transformation product that is not martensite; it should be emphasised that the optical micrograph for this condition is more representative of the amount of ferrite, whereas the scanning electron micrograph is taken deliberately to illustrate a region containing a substantial quantity of ferrite (Figs 3b,c). Small amounts of ferrite could be detected even for the 30% strain, 500 °C condition (Fig. 3c) and the 50% strain, 600 °C sample. The results are consistent with the longer time for the initiation of isothermal transformation at 600 °C (Fig. 1).

The hardness data for the untempered samples, in Fig. 4a, correlate with the microstructural observations, with 500 °C ausformed samples being consistently softer due to the unintended isothermal transformation products in the microstructure. However, there may be an additional factor, the occurrence of retained austenite due to the mechanical stabilisation described earlier. Fig. 4b shows that the slight softening of the sample ausformed at 600 °C to a 50% nominal strain might be explained in terms of its substantial retained austenite content. In order to prove this conjecture, the same samples were cooled in liquid nitrogen for 10 min in order to stimulate the austenite to decompose, but as can be seen from Fig. 4b, the cryogenic treatment did not result in the

---

[1]   The effective strain is given by

$$\frac{\sqrt{2}}{3}[(\epsilon_1 - \epsilon_2)^2 + (\epsilon_2 - \epsilon_3)^2 + (\epsilon_3 - \epsilon_1)^2]^{1/2} \tag{1}$$

where ϵ_i, $i = 1, 2, 3$ represent the principal strains calculated using the finite element method.
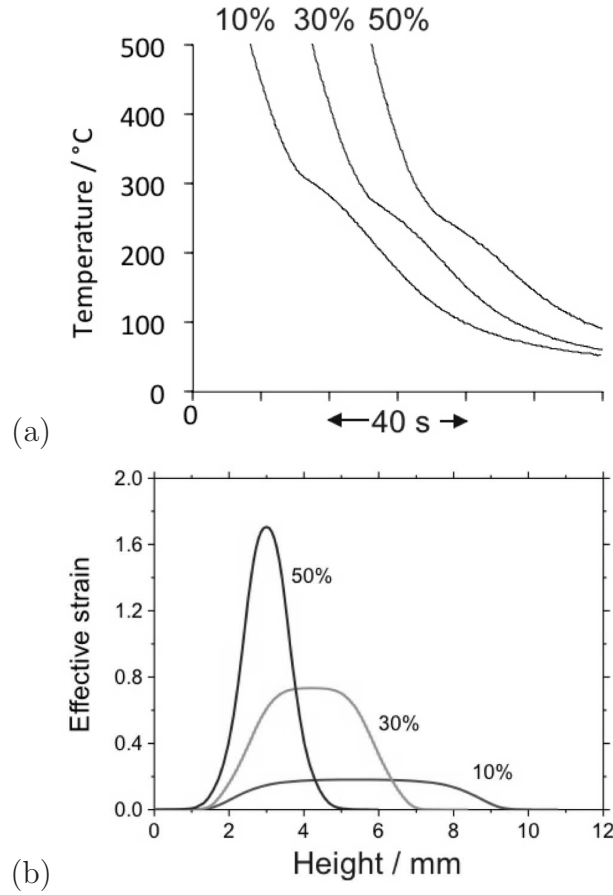
Fig. 2. (a) Cooling curves for the three samples, illustrating the changes in natural cooling when martensite forms. Two of the curves have been displaced along the horizontal axis by adding 10 and 20 s respectively, for clarity. (b) Calculated effective strain as a function of the nominal compression.

decomposition of the retained austenite. It is speculated that this is because the plastically deformed austenite is mechanically stabilised.

In low-alloy steels the laths of martensite tend to cluster together, and are organised hierarchically into blocks and packets within a given austenite grain [23]. A block consists of laths that are in virtually identical orientation in space, whereas a packet is the cluster of blocks which share the same austenite {111} close-packed plane to which the corresponding {011} martensite plane is almost parallel. The laths within a packet therefore have habit planes which make small angles with respect to each other, but have different crystallographic orientations. Those within blocks also have similar crystallographic orientations. It is important in the context of refinement, therefore, to reduce the block size. Figs. 5a-c show representative orientation maps for samples ausformed at 500 °C, and Fig. 5d shows an example of the evaluated block widths; it is interesting that the misorientation of 60° between adjacent blocks is consistent with the literature and expectations from the common γ/α' orientation

(a) Not deformed

(b) 500 °C, 50%

(c) 500 °C, 10%

(d) 500 °C, 30%

(e) 500 °C, 50%

(f) 600 °C, 10%
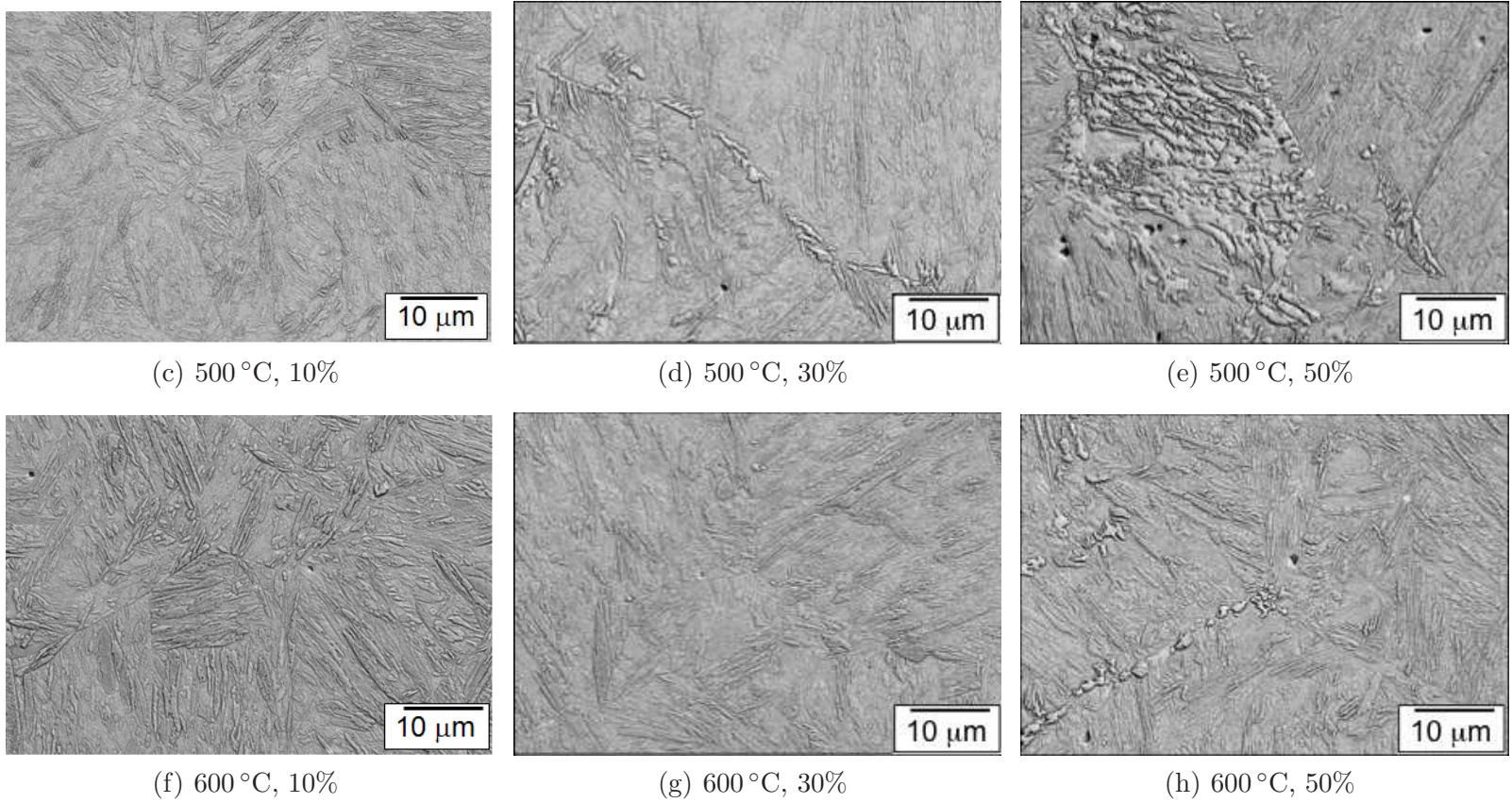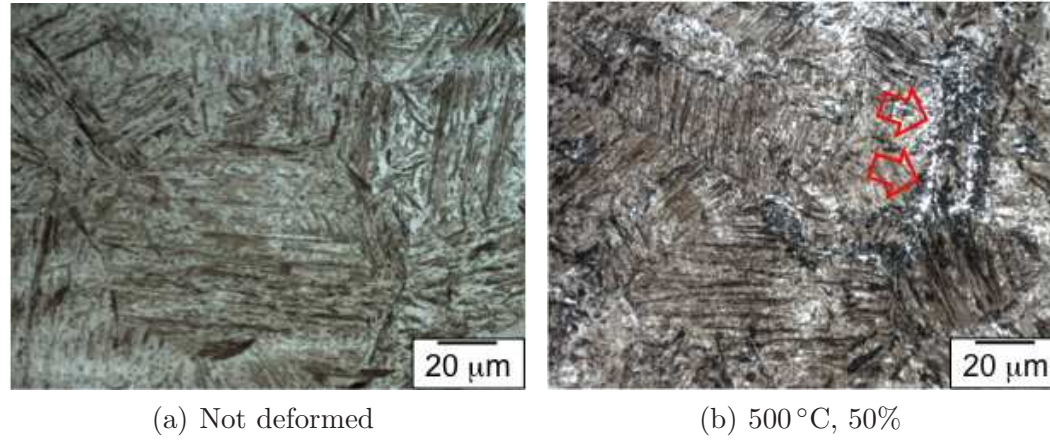
(g) 600 °C, 30%

(h) 600 °C, 50%

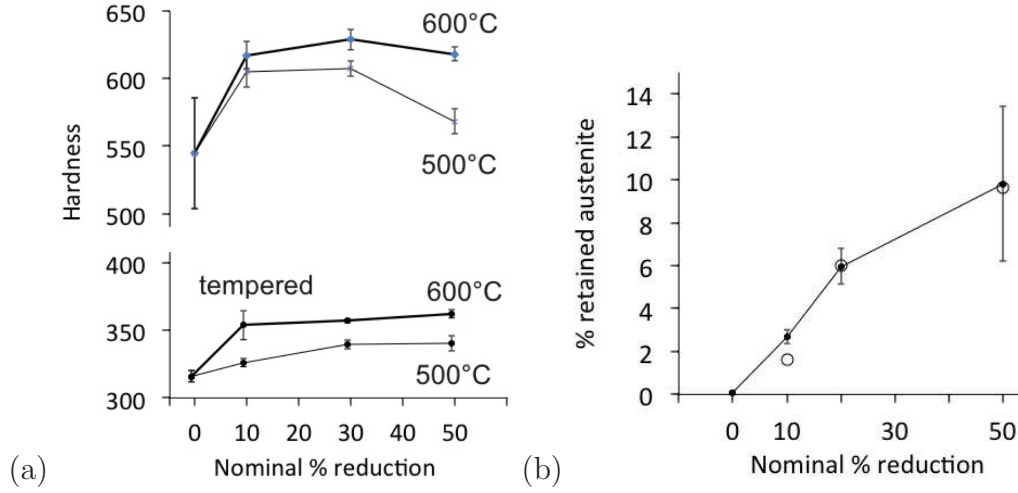Fig. 3. Optical (a,b) and scanning electron micrographs (c-h).

Fig. 4. (a) Hardness data for as-quenched and ausformed samples; the temperatures are those at which the deformation was carried out. The lower curves represent data following the tempering treatment at 550 °C for 90 min. (b) Retained austenite content after quenching (line) and following cooling in liquid nitrogen (points).

relationships [24]. The influence of ausforming condition on the block width of martensite for all the conditions is shown in Fig. 5f. The block width becomes smaller at greater reduction ratios, similar to trends reported in the case of 18Ni maraging steels even though the original block width of maraging steel is much larger [25]. In fact the mean block size at 50% nominal reduction at 500 °C is of the order of just 1 μm, a reduction by a factor of 3 when compared with the as-quenched martensite. It should be noted that the block sizes were measured on the tempered samples to ensure a high quality of orientation imaging; it is assumed that in the absence of recrystallisation, the block size does not change on tempering.

The changes in hardness of the ausformed samples are shown in Fig. 4a. In both as-quenched and tempered conditions, the martensite hardness is increased substantially by the deformation of austenite. The change expected through the refinement of the blocks can be estimated using an equation derived here from experimental data on Fe-0.2C-2Mn wt% steel [26]:

$$\sigma_L = 723 \times (2L)^{-1/2} + 784 \quad \text{MPa}, \qquad \text{with} \qquad \text{HV} \cong \sigma_L \times \frac{3}{9.81} \qquad (2)$$

where L is the block width and σ_L the corresponding strengthening. The largest reduction in block size relative to the undeformed sample occurs for the 10% nominal reduction at 500 °C, from about 3 to 1.5 μm, with a corresponding increase in measured hardness from 545 to 605 HV, of 60 HV. In contrast, the change in hardness expected using equation 2 is only 37 HV, showing that that the block size is only one of the factors influencing the increase in the strength of the ausformed steel. The discrepancy is most likely due to changes in dislocation density as illustrated in Fig. 6 which shows the

7

same general trends for the sample ausformed at $600\,^\circ$C as does the hardness in Fig. 4. In fact the change in dislocation density from $6.08 \times 10^{15}\,\mathrm{m}^{-2}$ in the as-quenched condition, to $1.17 \times 10^{16}\,\mathrm{m}^{-2}$ for the $600\,^\circ$C 10% nominal strain sample, is estimated using equation 14.16 of [4] to lead to an increase in hardness of $120\,\mathrm{HV}$. This is about 30% greater than observed (Fig. 4a), but the inevitable conclusion is that much of the hardness change on ausforming in the present case depends on the resulting increase in the dislocation density of the martensite.

It is seen from the present work is that even though ausforming results in substantial increases in hardness, the effect is substantially reduced on tempering under conditions appropriate for fasteners, Fig. 4a. Nevertheless, a hardness increase of about $50\,\mathrm{HV}$ can be obtained using ausforming.

(a) Undeformed   (b) $500\,^\circ$C, 10% (c) $500\,^\circ$C, 30%

(d) $500\,^\circ$C, 50% (e) $500\,^\circ$C, 50% (f) Block size
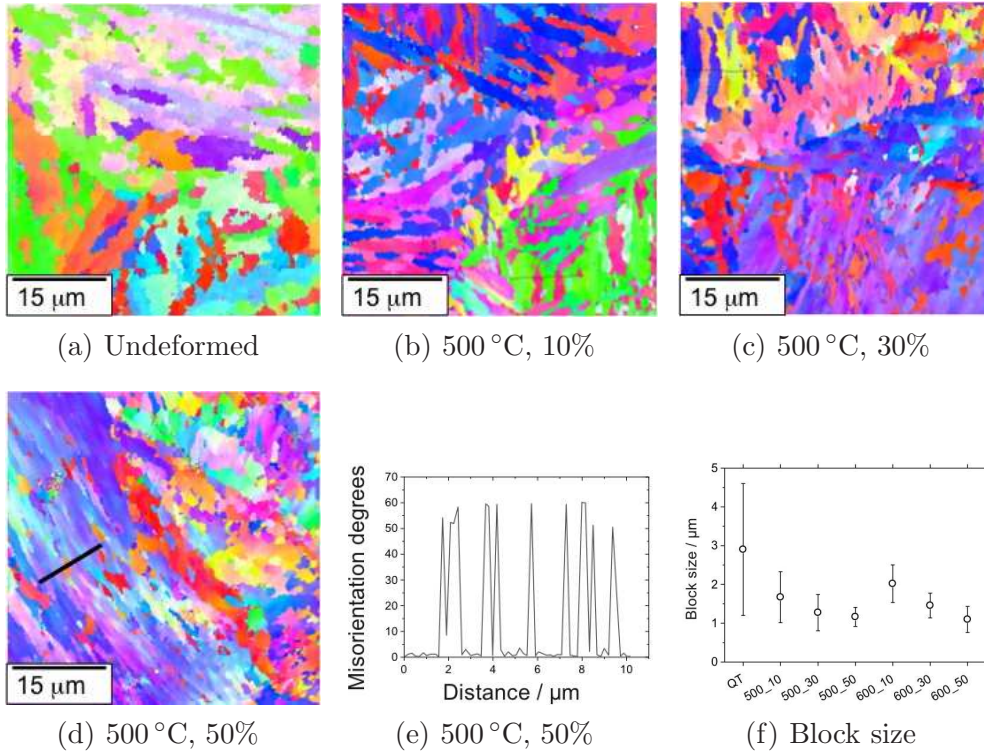
Fig. 5. Orientation images and corresponding data from quenched and tempered samples. Part (e) represents measurements done across the line in (d). The block sizes reported for the $500\,^\circ$C samples may be influenced by the presence of the small fraction of ferrite generated during ausforming.

5   Mechanical stabilisation

While the hardness results are in essence consistent with the earlier work on high-alloy steels [1], there are distinguishing features. Ausforming at lower temperatures generally leads to greater hardness unless other transformations
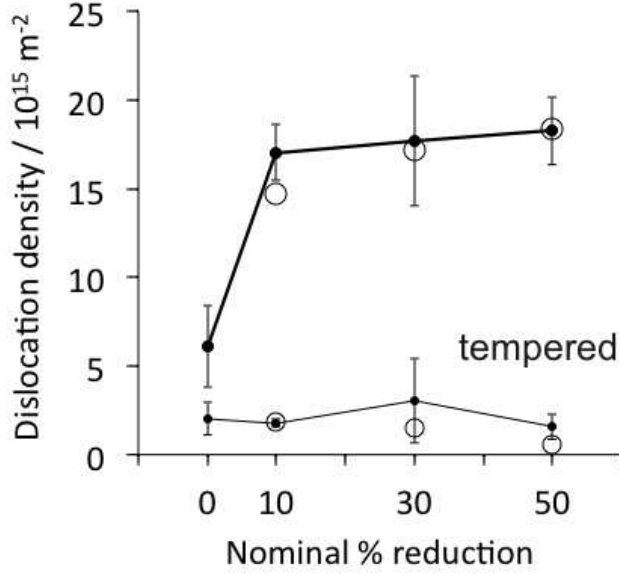
Fig. 6. Dislocation density data for the quenched, and quenched and tempered samples, measured using X-ray diffraction. (a) Lines and filled points for samples ausformed at 600 °C, (b) open circles for those ausformed at 500 °C; scatter bars are not presented for this case because of insufficient measurements.

intervene [1, 27]. However, Fig. 4a shows that the hardness of alloy ausformed at 500 °C is less than that at 600 °C following quenching to ambient temperature, because of the formation of ferrite during processing at 500 °C. Furthermore, the hardness increases at first as a function of the reduction ratio and then it decreases. Fig. 4b shows for the 600 °C condition where the structure during hot-deformation retains austenite, that the amount of retained austenite increases with the reduction ratio, explaining the softening at large reductions.

This is a reflection of the fact that the plastic deformation of austenite can mechanically stabilise it and reduce the amount of martensite that is ultimately obtained, consistent with the suppression of the martensite-start temperature descried in section 3. The theory for estimating the onset of mechanical stabilisation relies on balancing the force driving the motion of the interface against the resistance of the dislocation debris created by the deformation of the austenite [28, 29]. This theory can also be used to estimate quantitatively the suppression of the M_S temperature [30].

The M_S temperature is calculated from the free energy change $\Delta G^{\gamma\alpha'} = G_{\alpha'} - G_\gamma$ for the transformation of austenite to martensite reaching a critical value $\Delta G^{\gamma\alpha}_{M_S}$. Plastic strain through mechanical stabilisation introduces an additional driving force ΔG_{STA} needed in order for the interface to overcome the dislocation density (ρ) in the austenite, created by strain prior to transformation [28, 29]:

$$\Delta G_{STA} = \frac{\mu b}{8\pi(1-\nu)}(\rho^{0.5} - \rho_0^{0.5}) \qquad \mathrm{J\,m^{-3}}$$

$$\text{with} \qquad \rho = 2 \times 10^{13} + 2 \times 10^{14}\epsilon \qquad \mathrm{m^{-2}} \qquad (3)$$

9

where μ is the shear modulus of austenite at $80\,\mathrm{GPa}$, $b = 0.252\,\mathrm{nm}$ is the magnitude of the Burgers vector of the dislocations, and the Poisson's ratio $\nu = 0.27$. The martensite–start temperature is obtained from [2]

$$\Delta G^{\gamma\alpha} < \Delta G_{M_S}^{\gamma\alpha} - \Delta G_{STA} \tag{4}$$

The resulting calculations, together with data derived from Fig. 2 are listed in Table 1. The small stress that was maintained constant following the application of the deformation was also accounted for in the calculations as described in [30, 31]. There is a correlation between the measured and calculated data, although the latter values are always larger. This is because the M_S measured from the cooling curves is dependent on the deviation from natural cooling caused by the heat of transformation, so the first-detectable transformation probably corresponds to a substantial amount of transformation. But the results reinforce the conclusion regarding the mechanical stabilisation when martensitic transformation occurs from plastically deformed austenite.

Table 1
Calculated and measured martensite-start temperatures.

Nominal % strain	Effective strain	Stress / MPa	Measured M_S / °C	Calculated M_S / °C
0	0	0	359	
10	0.17	2	350	355
30	0.70	20	332	347
50	1.70	31	280	331

6 Transmission electron microscopy

Molybdenum carbides could not be detected in the ausformed state, either because they are very fine and difficult to image in the heavily dislocated martensite in the final structure, but in fact the deformation times are in the range 0.01-0.05 s so precipitation may not be expected during ausforming (Fig. 7a). However, differences were found in the cementite precipitation behaviour between the as-quenched and tempered, and as-ausformed and tempered structures. Fig. 7b,c show the microstructures following tempering and

---

[2] The computer program capable of the calculations presented here can be downloaded freely from

http://www.msm.cam.ac.uk/map/steel/programs/mucg46B.htm

it is evident that the cementite is finer in the sample with the nominal strain of 30%. Quantitative measurements indicated that the cementite size was refined from $131 \pm 51\,\mu m$ to $98 \pm 42\,\mu m$ on increasing the ausforming reduction from 10% to 30% (the size uncertainties are standard deviations in the data). This refinement of cementite particle size cannot be attributed to increased dislocation density the difference between these two conditions is not large (Fig. 6). However, it is clear that the 30% strain sample has more intense precipitation at the martensite plate boundaries. This would be precipitation to occur followed by intragranular precipitation, because boundaries are more effective nucleation sites than dislocations. As a consequence, less carbon would be available for intragranular precipitation, leading to finer particle sizes.

So the question remains, why has precipitation focused on the boundaries for the more intensely ausformed sample? When martensite forms in deformed austenite, the structure of the α'/γ boundaries will be more imperfect than when it forms in perfect austenite. This is because many of the extrinsic dislocations will be incorporated in the transformation interfaces, which eventually are halted in their progress by mechanical stabilisation. Such boundaries would therefore have a higher energy and become more effective nucleation sites.

7 Conclusions

Experiments have been conducted to study the ausforming response of a low-alloy steel that is used in the manufacture of fasteners. As a result, the following conclusions can be reached:

(1) It is possible with rapid deformation in the bay region of the time-temperature-transformation diagram, to impart sufficient deformation to the austenite without causing unwanted transformation, so that on quenching the structure obtained is substantially harder.
(2) The increase in the hardness of the martensite that grows in deformed austenite is mainly due to an increased dislocation density, rather than the refinement of the microstructure.
(3) The gain in hardness and dislocation density due to ausforming is most pronounced when the extent of deformation is just 10% in compression, with increasing deformations giving diminishing returns.
(4) There is clear evidence that deformed austenite becomes more resistant to martensitic transformation as the level of deformation is increased, both in terms of the suppression of the martensite-start temperature and the retention of austenite.
(5) Fasteners are subjected to severe tempering following quenching; the effect of this is to eliminate many of the differences between the quenched-and-tempered, and ausformed-quenched-and-tempered samples. Never-

11

theless, hardness increases of about 50 HV can still be obtained relative to samples that are not subjected to ausforming.
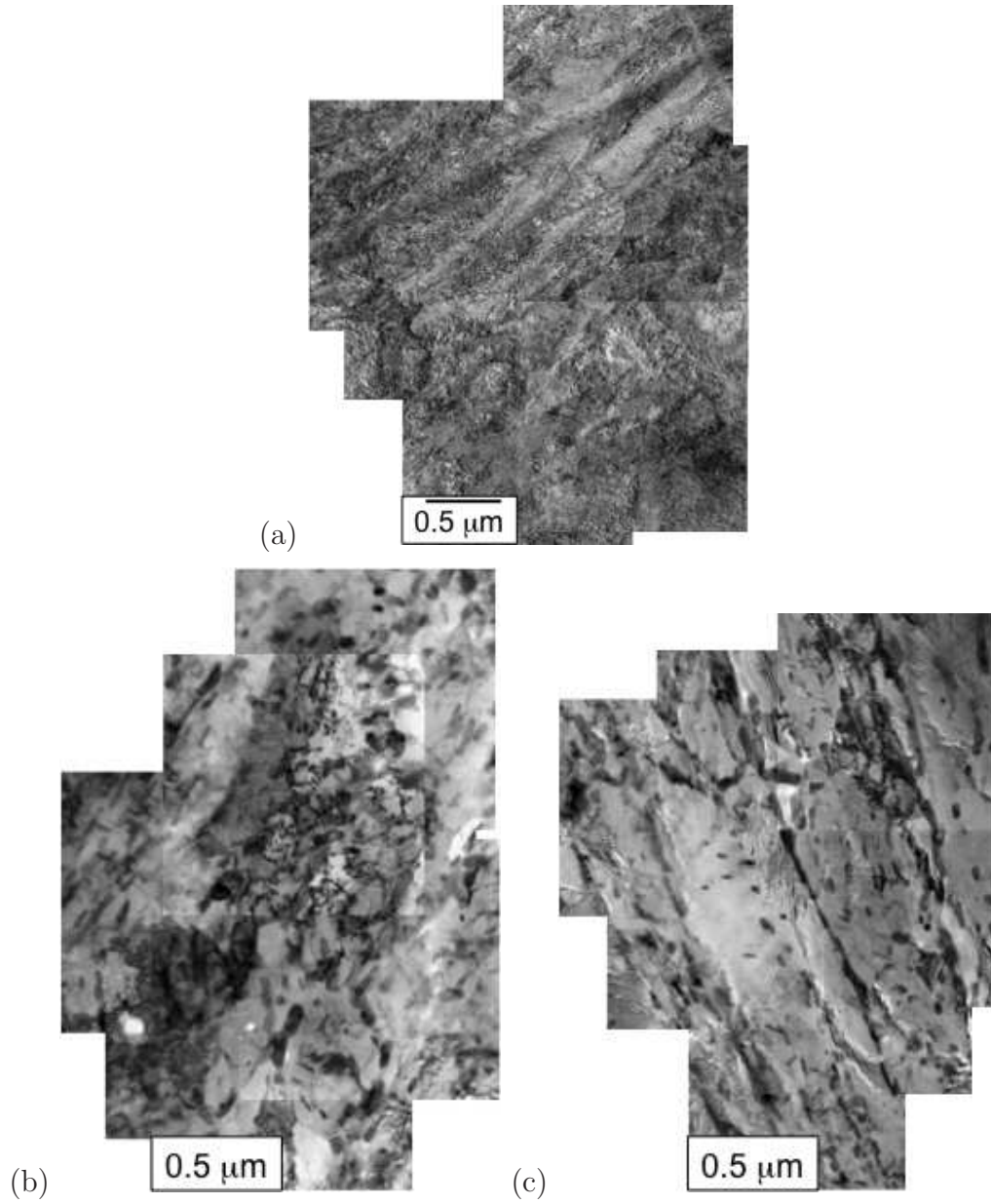
(a)

(b)   (c)

Fig. 7. TEM of sample ausformed at 500 °C. (a) Quenched after ausforming to 30% nominal strain. (b) Ausformed to a nominal strain of 10%, quenched and tempered. (c) As (b) but a nominal strain of 30%.

12

References

1. D. J. Schmatz, and V. F. Zackay: 'Mechanical properties of deformed metastable austenitic UHS steel', *Trans. ASM*, 1959, **51**, 476–494.

2. W. E. Duckworth, P. R. Taylor, and D. A. Leak: 'Ausforming behaviour of En24, En30B and an experimental 3%Cr-Ni-Si steel', *Journal of the Iron and Steel Institute*, 1964, **202**, 135–142.

3. G. Thomas, D. Schmatz, and W. Gerberich: 'Structure and strength of some ausformed steels', In: V. F. Zackay, ed. *High Strength Materials*. New York, USA: John Wiley & Sons, Inc., 1965:251–326.

4. R. W. K. Honeycombe, and H. K. D. H. Bhadeshia: Steels: Microstructure and Properties, 2nd edition: Butterworths–Hienemann, London, 1995.

5. Y. Tomita: 'Development of fracture toughness of ultrahigh strength, medium carbon, low alloy steels for aerospace applications', *International Materials Reviews*, 2000, **45**, 27–37.

6. H. E. Boyer, and A. G. Gray: Atlas of Isothermal Transformation and Cooling Transformation Diagrams: Metals Park, Ohio, USA: ASM, 1977.

7. M. Peet, and H. K. D. H. Bhadeshia: 'Software for transformations in steels': http://www.msm.cam.ac.uk/map/steel/programs/mucg83.html, 1982.

8. 'JMatPro - practical software for materials properties, http://www.sentesoftware.co.uk/': 2014: URL `http://www.sentesoftware.co.uk/`.

9. Y. Li, E. Onodera, and A. Chiba: 'Friction coefficient in hot compression of cylindrical sample', *Materials transactions*, 2010, **51**, 1210–1215.

10. S. Takebayashi, T. Kunieda, N. Yoshinaga, K. Ushioda, and S. Ogata: 'Comparison of the dislocation density in martensitic steels evaluated by some x-ray diffraction methods', *Isij International*, 2010, **50**, 875–882.

11. T. Ungár, and A. Borbély: 'The effect of dislocation contrast on X-ray line broadening: A new approach to line profile analysis', *Applied Physics Letters*, 1996, **69**, 3173–3175.

12. A. R. Stokes: 'A numerical Fourier-analysis method for the correction of widths and shapes of lines on X-ray powder photographs', *Proceedings of the Physical Society*, 1948, **61**, 382–391.

13. E. S. Machlin, and M. Cohen: 'Burst phenomenon in the martensitic transformation', *Trans. Metall. Soc. AIME*, 1951, **191**, 746–754.

14. H. C. Fiedler, B. L. Averbach, and M. Cohen: 'The effect of deformation on the martensitic transformation', *Transactions of the American Society for Metals*, 1955, **47**, 267–290.

15. W. C. Leslie, and R. L. Miller: 'The stabilization of austenite by closely spaced boundaries', *ASM Transactions Quarterly*, 1964, **57**, 972–979.

16. J. R. Strife, M. J. Carr, and G. S. Ansell: 'Effect of austenite prestrain above the M_d temperature on the M_s temperature in Fe-Ni-Cr-C alloys', *Metallurgical Transactions A*, 1977, **8A**, 1471–1484.

17. K. Tsuzaki, S. Fukasaku, Y. Tomota, and T. Maki: 'Effect of prior defor-

mation of austenite on the gamma-epsilon martensitic transformation in Fe-Mn alloys', *Trans. JIM*, 1991, **32**, 222–228.

18. V. Raghavan: 'Kinetics of martensitic transformations', In: G. B. Olson, and W. S. Owen, eds. *Martensite*. Ohio, USA: ASM International, 1992:197–226.

19. A. Das, P. C. Chakraborti, S. Tarafder, and H. K. D. H. Bhadeshia: 'Analysis of deformation induced martensitic transformation in stainless steels', *Materials Science and Technology*, 2011, **27**, 366–370.

20. S. M. C. van Boheman, and J. Sietsma: 'Kinetics of martensite formation in plain carbon steels: critical assessment of possible influence of austenite grain boundaries and autocatalysis', *Materials Science and Technology*, 2014, **?**, DOI 10.1179/1743284714Y.0000000532.

21. A. Mangal, P. Biswas, S. Lenka, V. Singh, S. B. Singh, and S. Kundu: 'Dilatometric and microstructural response of variant selection during martensitic transformation', *Materials Science and Technology*, 2014, **?**, DOI: http://dx.doi.org/10.1179/1743284713Y.0000000487.

22. H. K. D. H. Bhadeshia: Bainite in Steels, 2nd edition: London, U.K.: Institute of Materials, 2001.

23. T. Maki: 'Microstructure and mechanical properties of ferrous martensites', *Materials Science Forum*, 1990, **56–58**, 157–168.

24. H. Kitahara, R. Ueji, N. Tsuji, and Y. Minamino: 'Crystallographic features of lath martensite in low-carbon steel', *Acta Materialia*, 2006, **54**, 1279–1288.

25. I. Tamura, K. Tsuzaki, and T. Maki: 'Morphology of lath martensite formed from deformed austenite in 18% ni maraging steel', *Journal de Physique Colloque*, 1982, **43**, 551–556.

26. S. Morito, X. Huang, T. Furuhara, T. Maki, and N. Hansen: 'The morphology and crystallography of lath martensite in alloy steels', *Acta Metallurgica*, 2006, **54**, 5323–5331.

27. K. S. Cho, J. H. Choi, H. S. Kang, S. H. Kim, K. B. Lee, H. R. Yang, and H. Kwon: 'Influence of rolling temperature on the microstructure and mechanical properties of secondary hardening high Co–Ni steel bearing 0.28 wt% C', *Materials Science & Engineering A*, 2010, **527**, 7286–7293.

28. S. Chatterjee, H. S. Wang, J. R. Yang, and H. K. D. H. Bhadeshia: 'Mechanical stabilisation of austenite', *Materials Science and Technology*, 2006, **22**, 641–644.

29. M. Maalekian, E. Kozeschnik, S. Chatterjee, and H. K. D. H. Bhadeshia: 'Mechanical stabilisation of eutectoid steel', *Materials Science and Technology*, 2007, **23**, 610–612.

30. H.-S. Yang, D. W. Suh, and H. K. D. H. Bhadeshia: 'More complete theory for the calculation of the martensite-start temperature in steels', *ISIJ International*, 2012, **52**, 162–164.

31. J. R. Patel, and M. Cohen: 'Criterion for the action of applied stress in the martensitic transformation', *Acta Metallurgica*, 1953, **1**, 531–538.